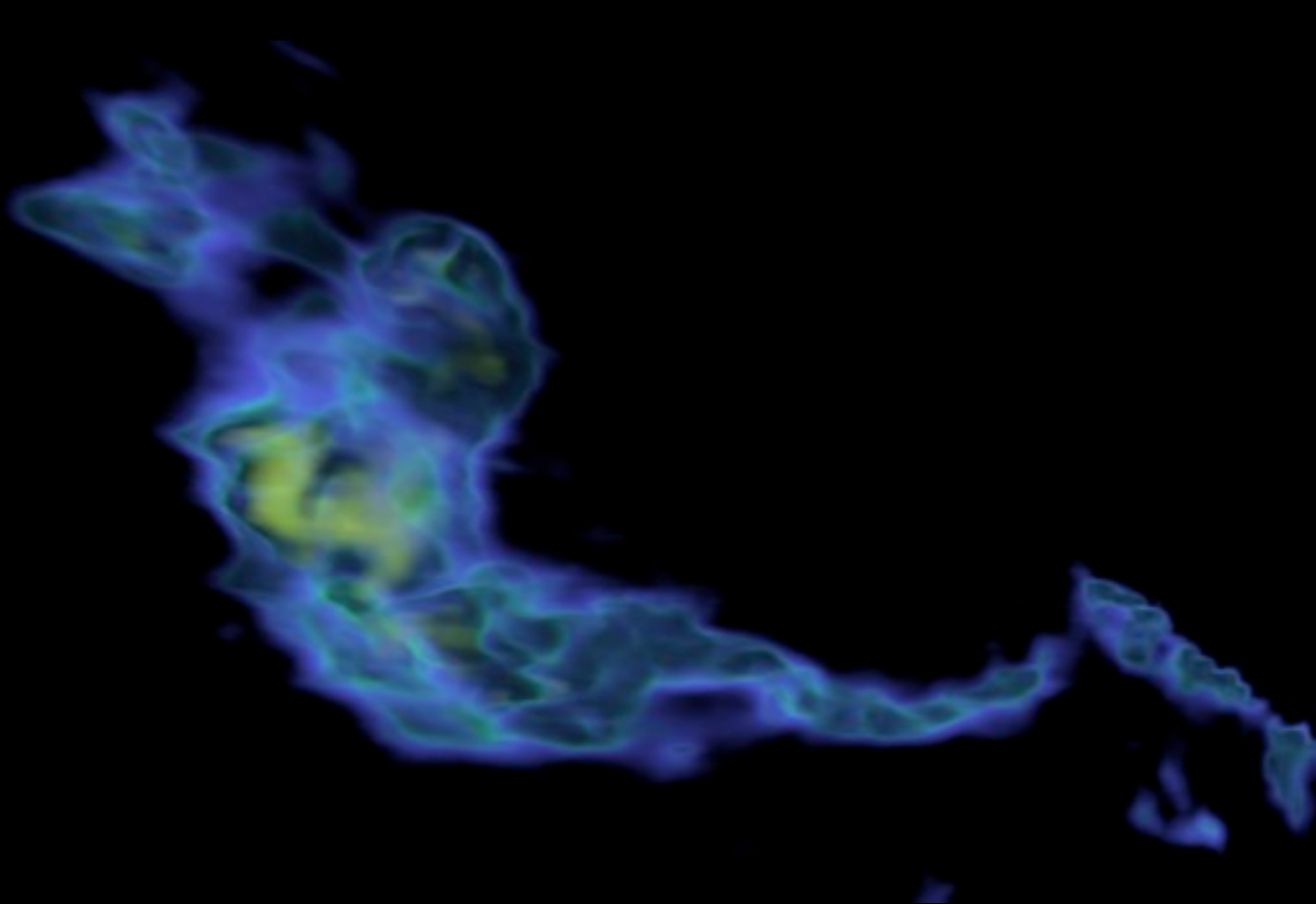


“Astronomical Medicine”

IIC Team: Douglas Alan, Michelle Borkin, Alyssa Goodman, Michael Halle, Jens Kauffman

A-M Collaborators: Jonathan Foster, Nick Holliman, Jaime Pineda, Erik Rosolowsky

Astronomy + Medicine = Understanding



Initiative in Innovative Computing @ Harvard
and

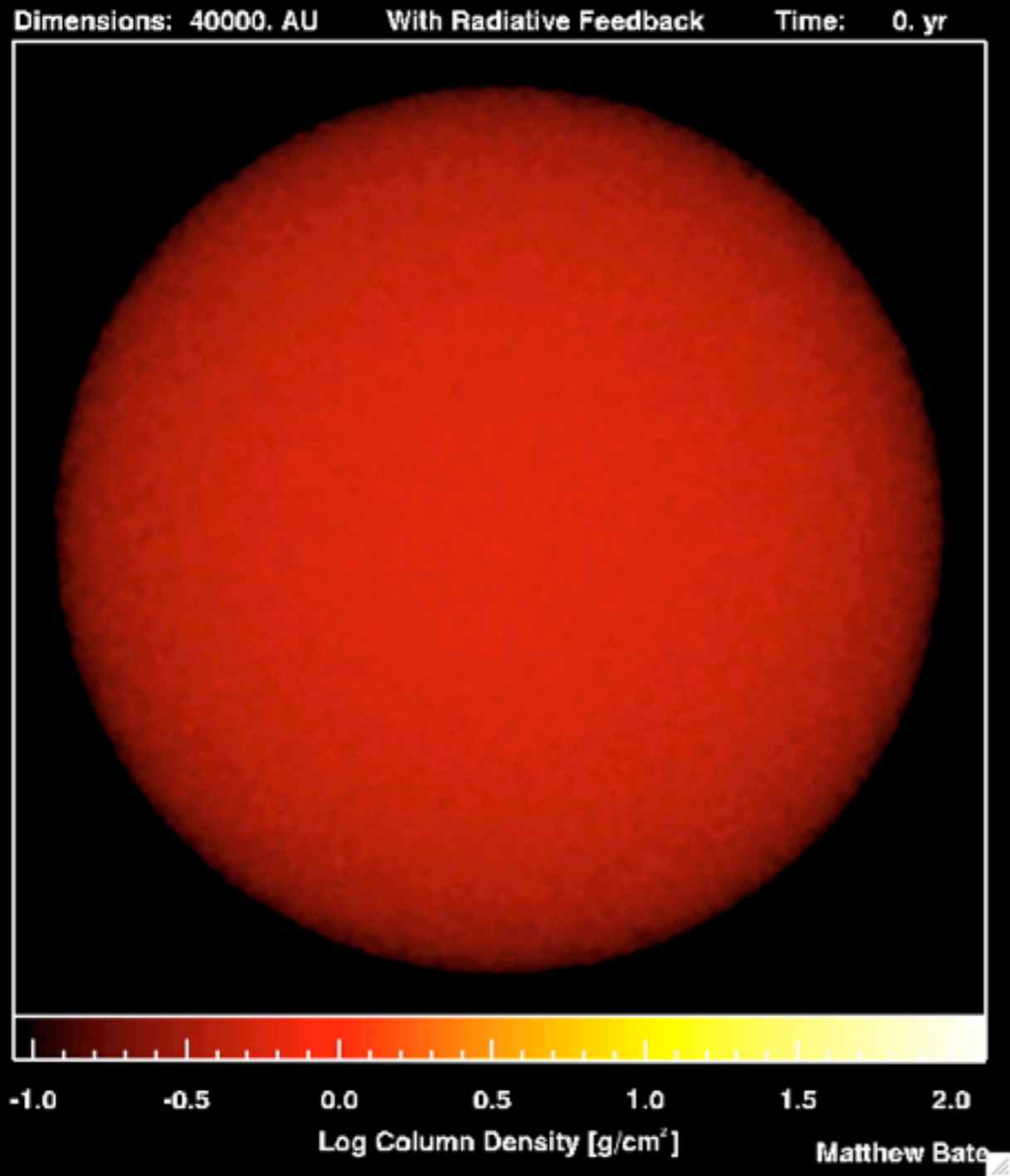


Harvard-Smithsonian Center for Astrophysics

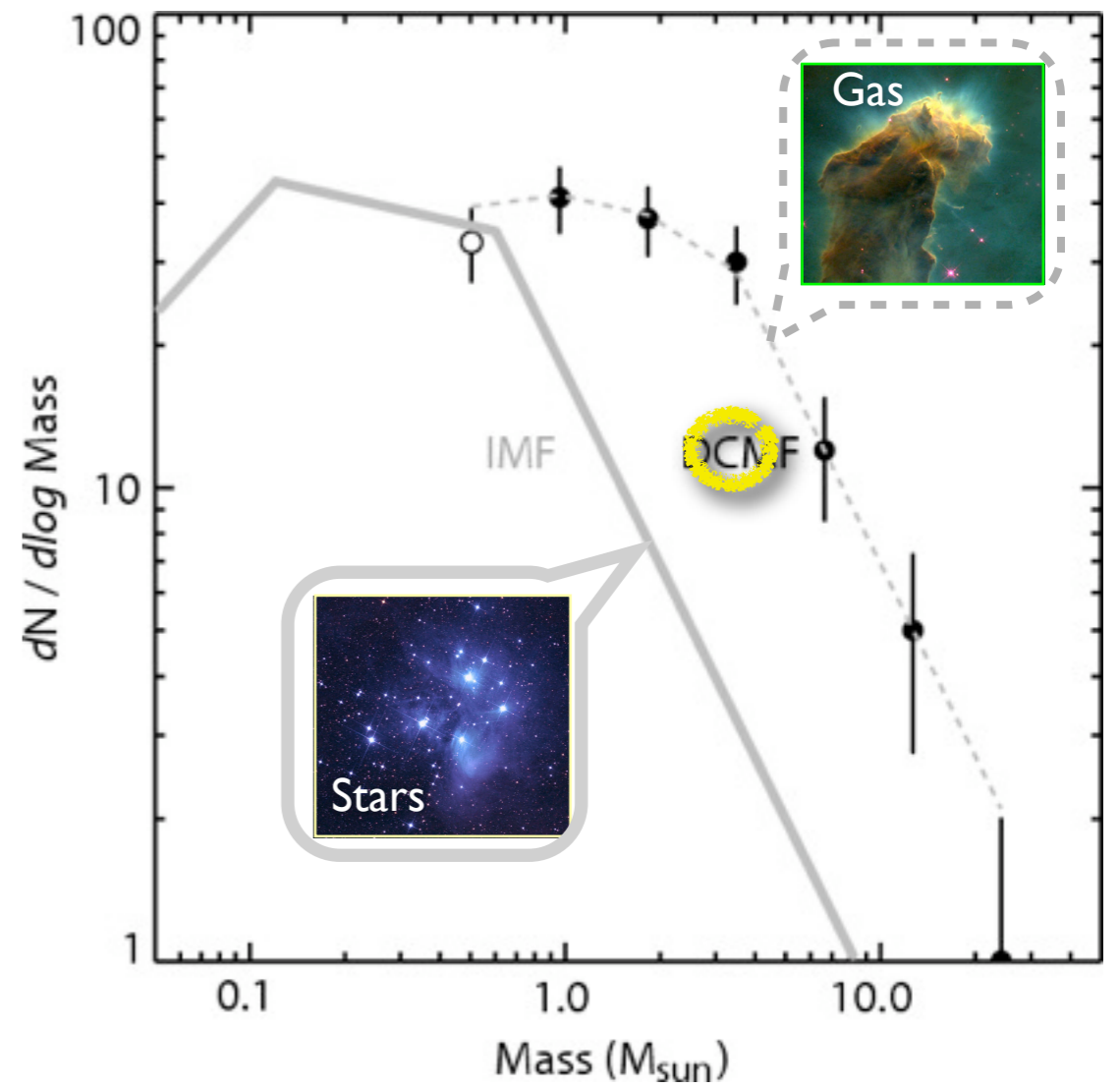
Monday, November 16, 2009

Left: I3CO in B5 in VolView, N. Holliman **Right:** Visualization of a DTI measurement of a human brain. Depicted are reconstructed fiber tracts that run through the mid-sagittal plane. Especially prominent are the U-shaped fibers that connect the two hemispheres through the corp. Rendering is own work, using a modified version of the BioTensor application developed at the University of Utah. The dataset is courtesy of Gordon Kindlmann at the Scientific Computing and Imaging Institute, University of Utah, and Andrew Alexander, W.M. Keck Laboratory for Functional Brain Imaging and Behaviour, University of Wisconsin, Madison. It is publicly available from [1]

From this ...to this?



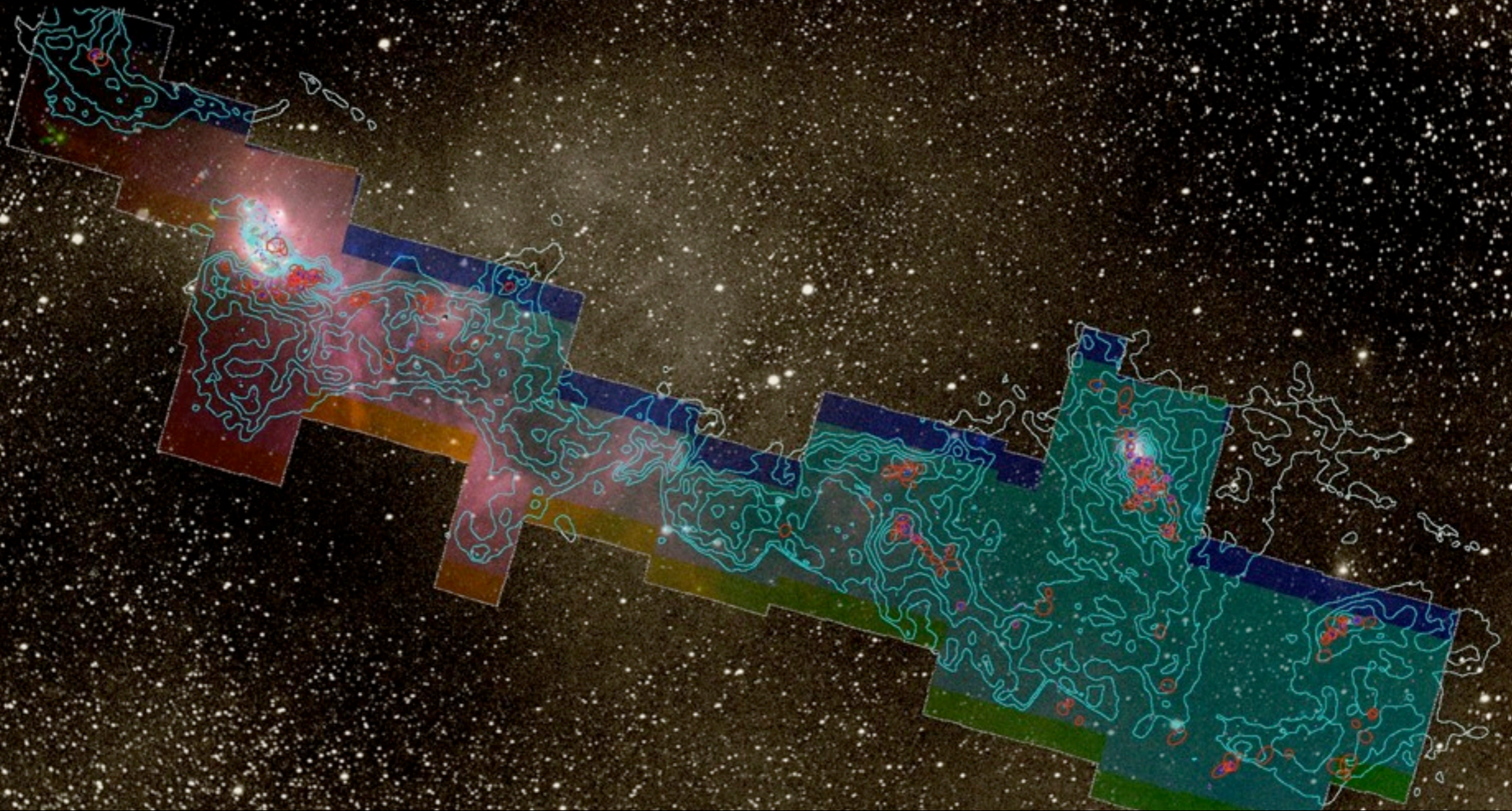
Bate 2009; cf. Padoan & Nordlund 2002



Alves, Lombardi & Lada 2007

COMPLETE

= **CO**ordinated **M**olecular **P**robe **L**ine **E**xinction **T**hermal
Emission Survey of Star-Forming Regions



COMPLETE Collaborators,
2009:

Alyssa A. Goodman (CfA/IIC)

João Alves (Calar Alto, Spain)

Héctor Arce (Yale)

Michelle Borkin (Harvard SEAS/IIC)

Paola Caselli (Leeds, UK)

James DiFrancesco (HIA, Canada)

Jonathan Foster (B.U.)

Mark Heyer (UMASS/FCRAO)

Doug Johnstone (HIA, Canada)

Jens Kauffmann (JPL/Caltech)

Helen Kirk (CfA)

Di Li (JPL/Caltech)

Stella Offner (CfA)

Jaime Pineda (CfA, PhD Student)

Thomas Robitaille (CfA)

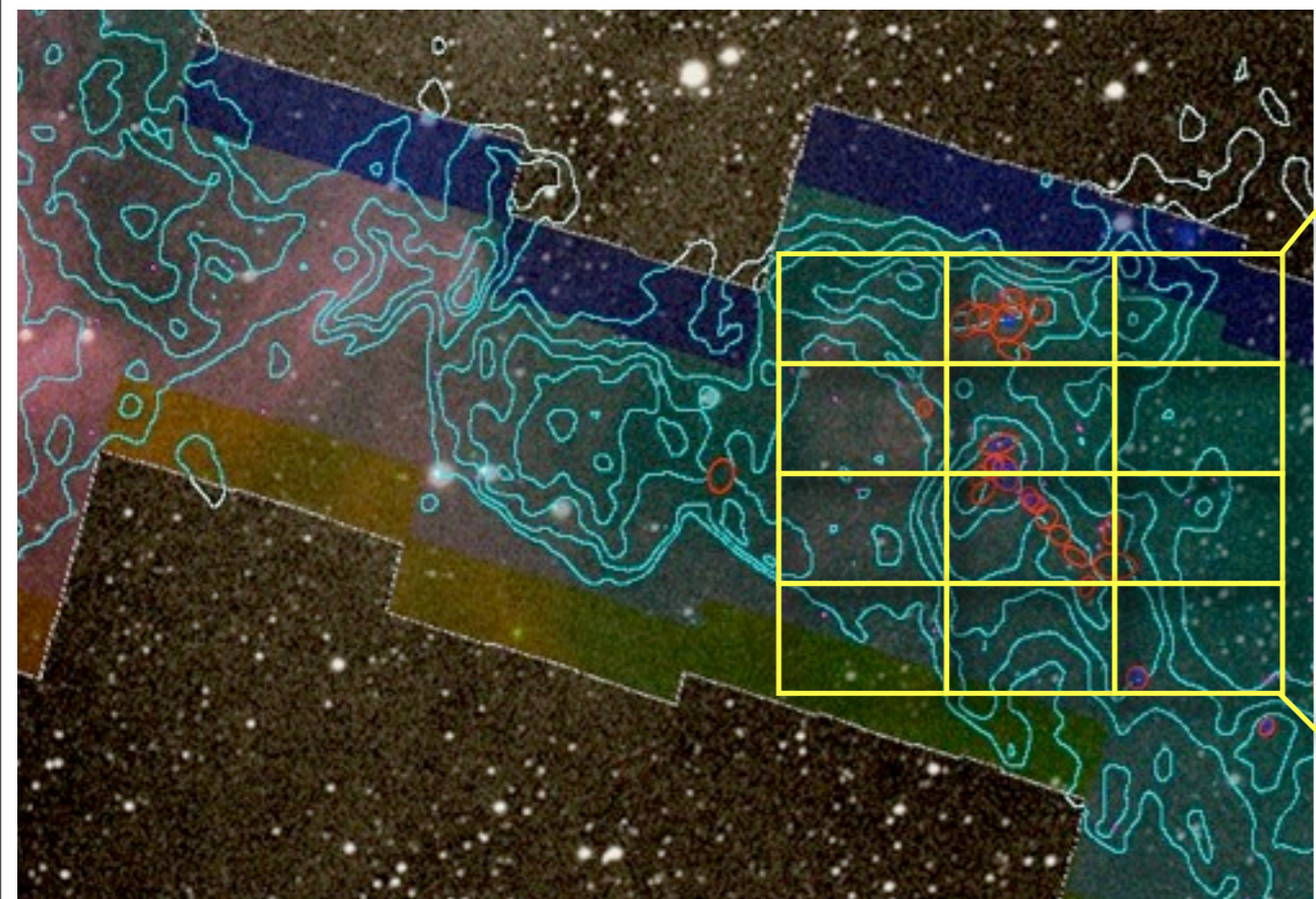
Erik Rosolowsky (UBC Okanagan)

Rahul Shetty (ITA Heidelberg)

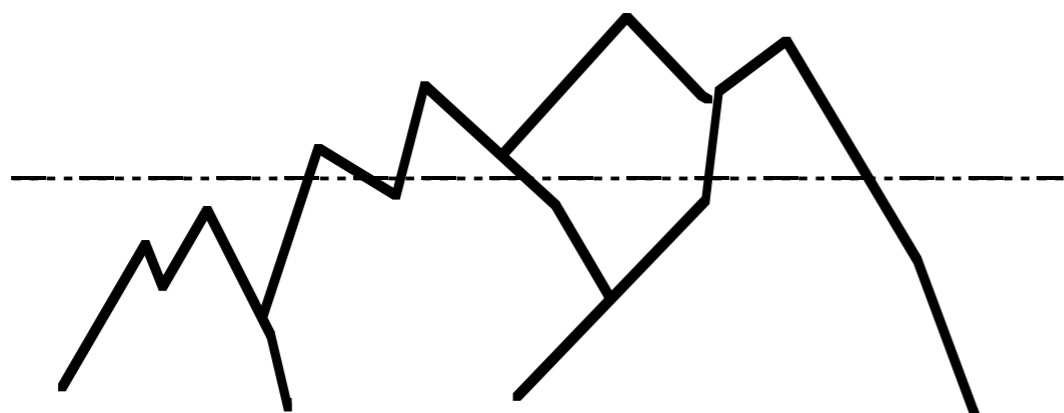
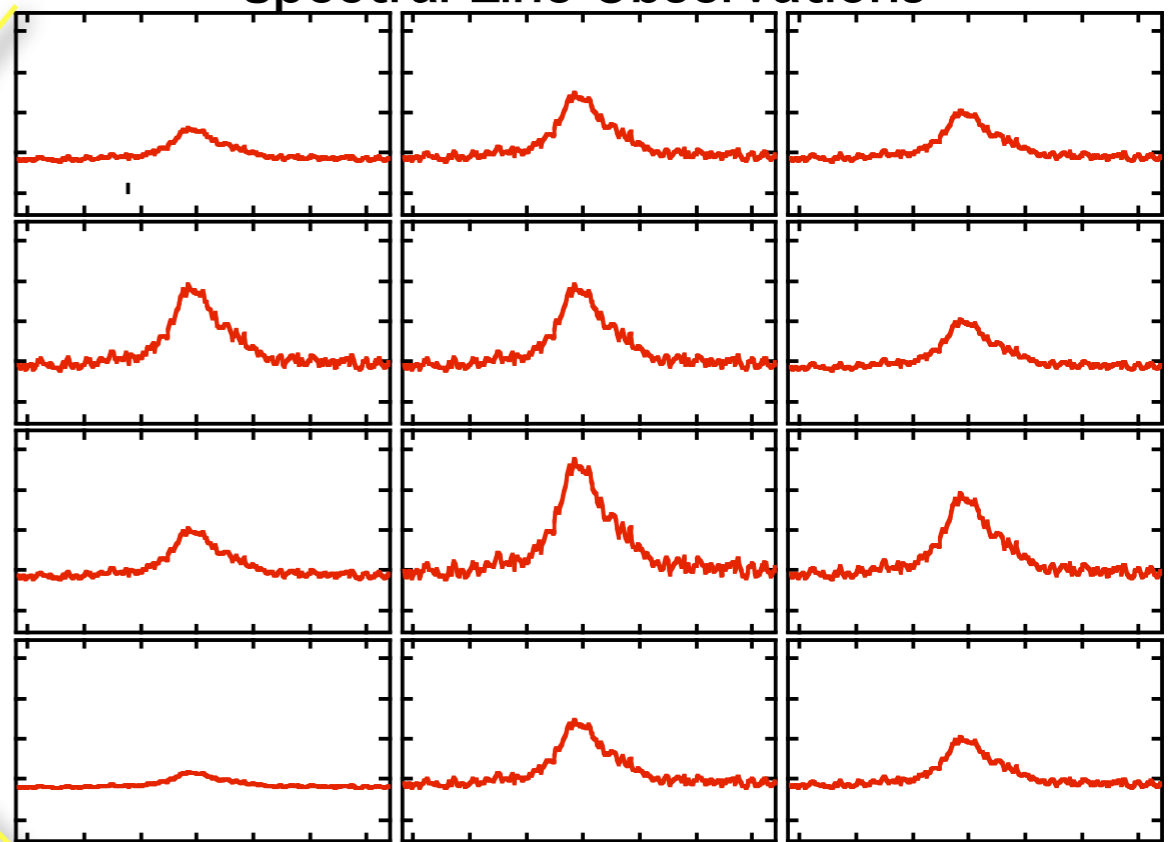
Scott Schnee (HIA Victoria)

Mario Tafalla (OAN, Spain)

There's much more to life than "integrated intensity"



Spectral Line Observations



Mountain Range



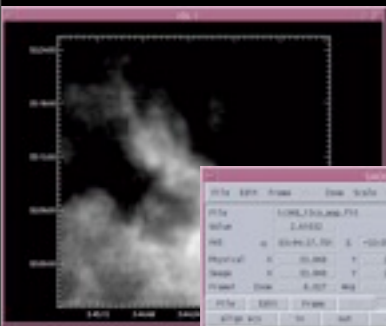
No loss of information



Loss of 1 dimension

Astronomical Visualization Tools are Traditionally 2D

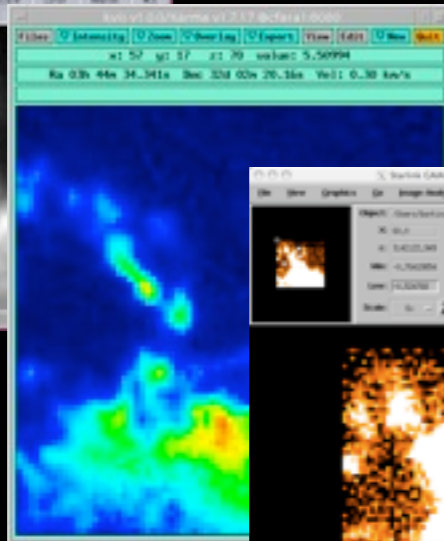
IDL



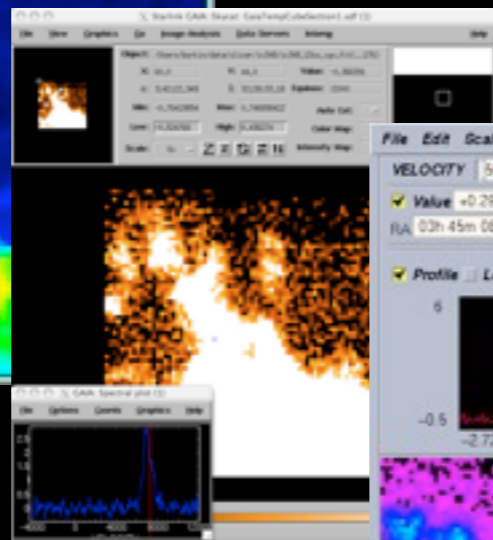
DS9



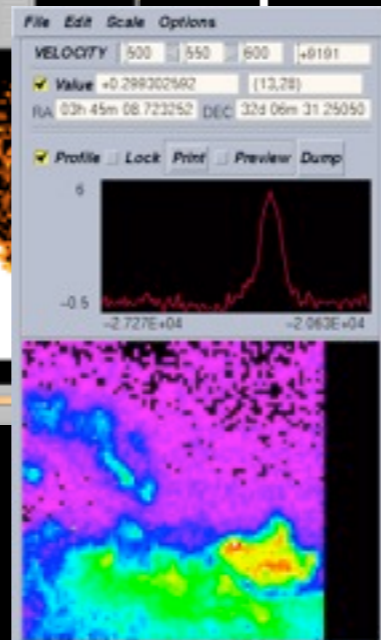
Karma*



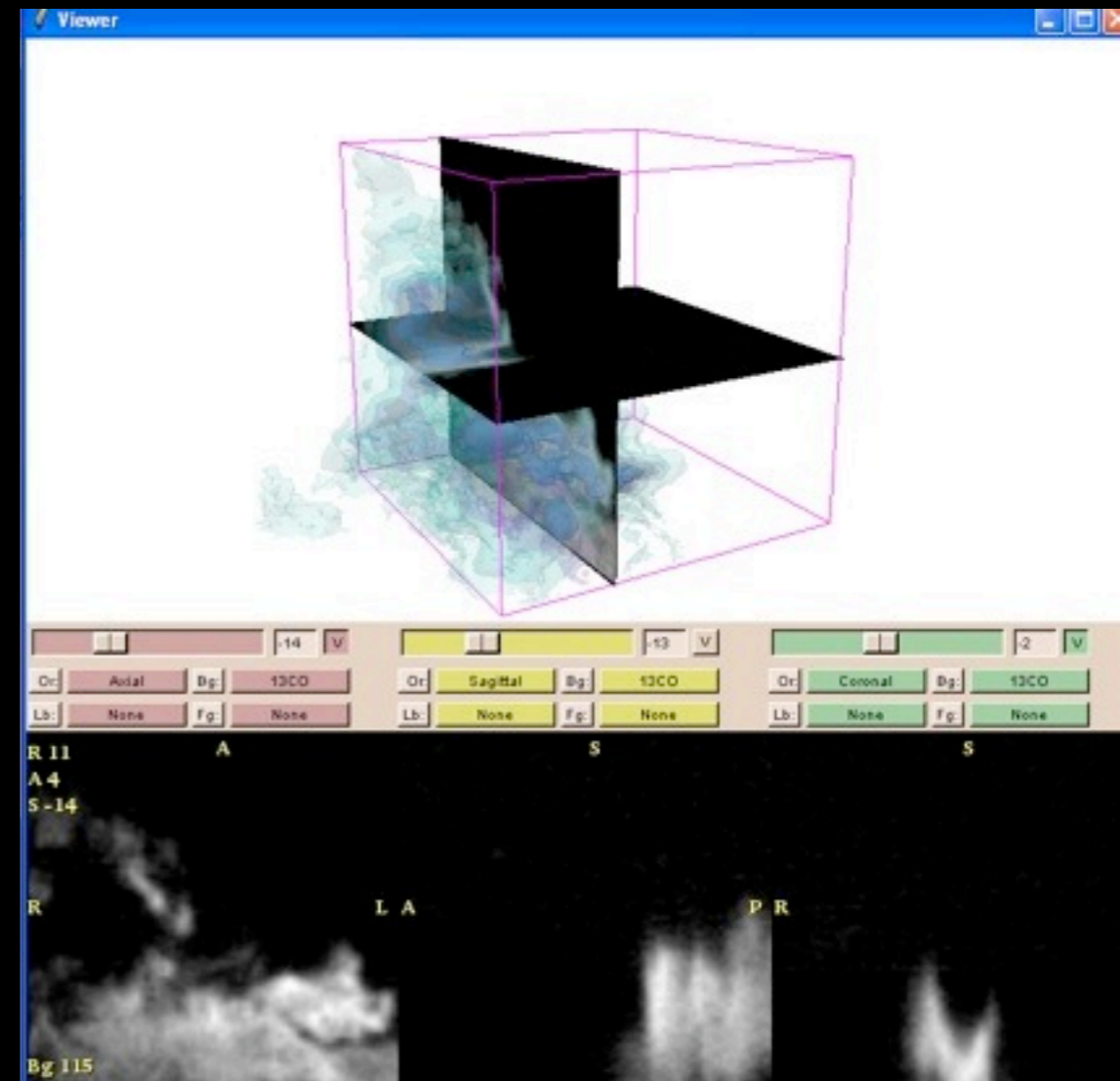
GAIA



Aipsview



3D Slicer



“3D”=movies (i.e. stepping through velocity)

Monday, November 16, 2009

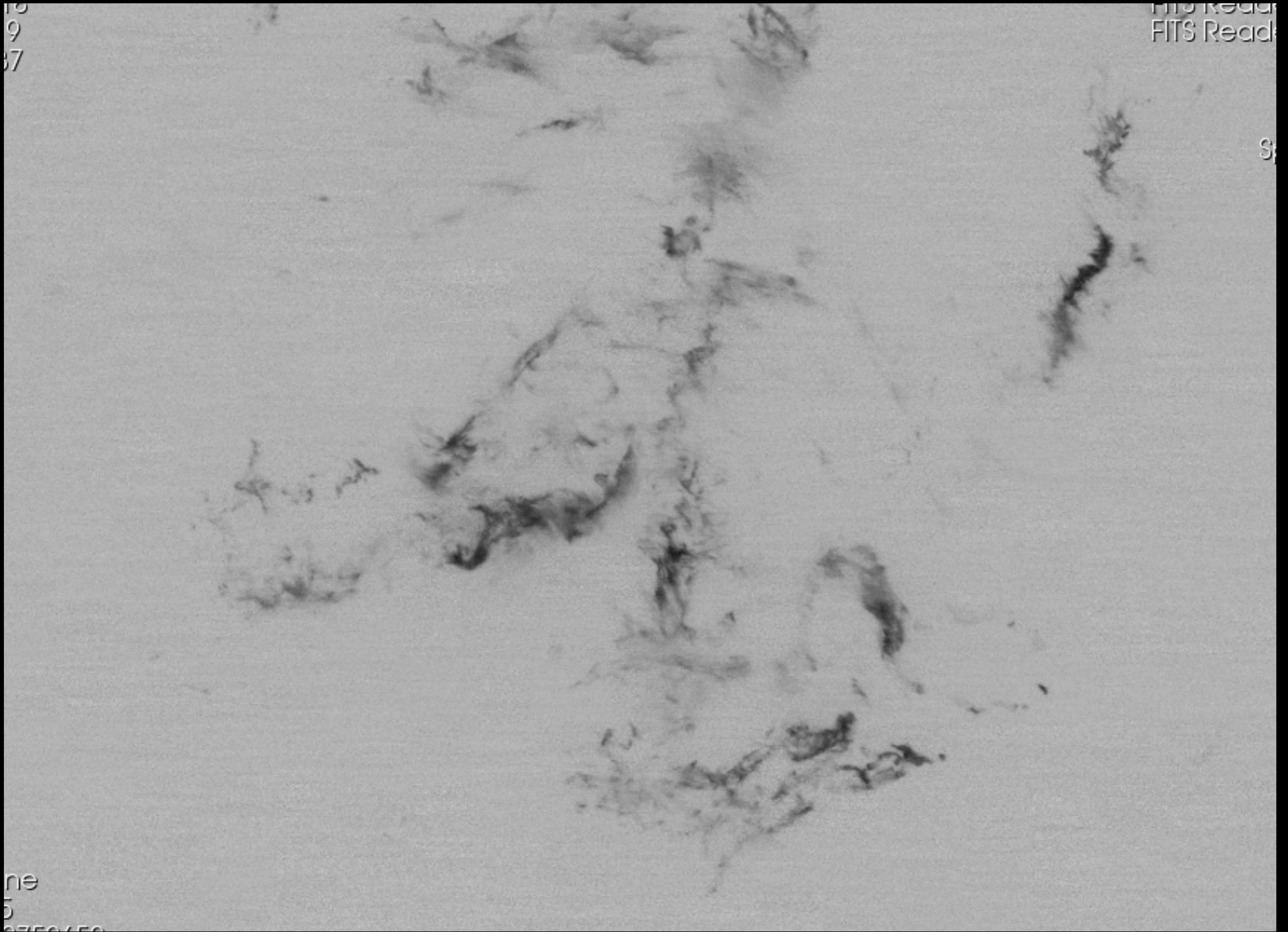
Challenge in displaying spectral line data cubes.

Hard to address all three dimensions at once, but made compact with 3D Slicer.

3D Slicer is a visualization tool taking fundamentally different approach.





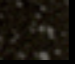
3D Slicer built and designed for 3D viewing; others come from 2D approach.

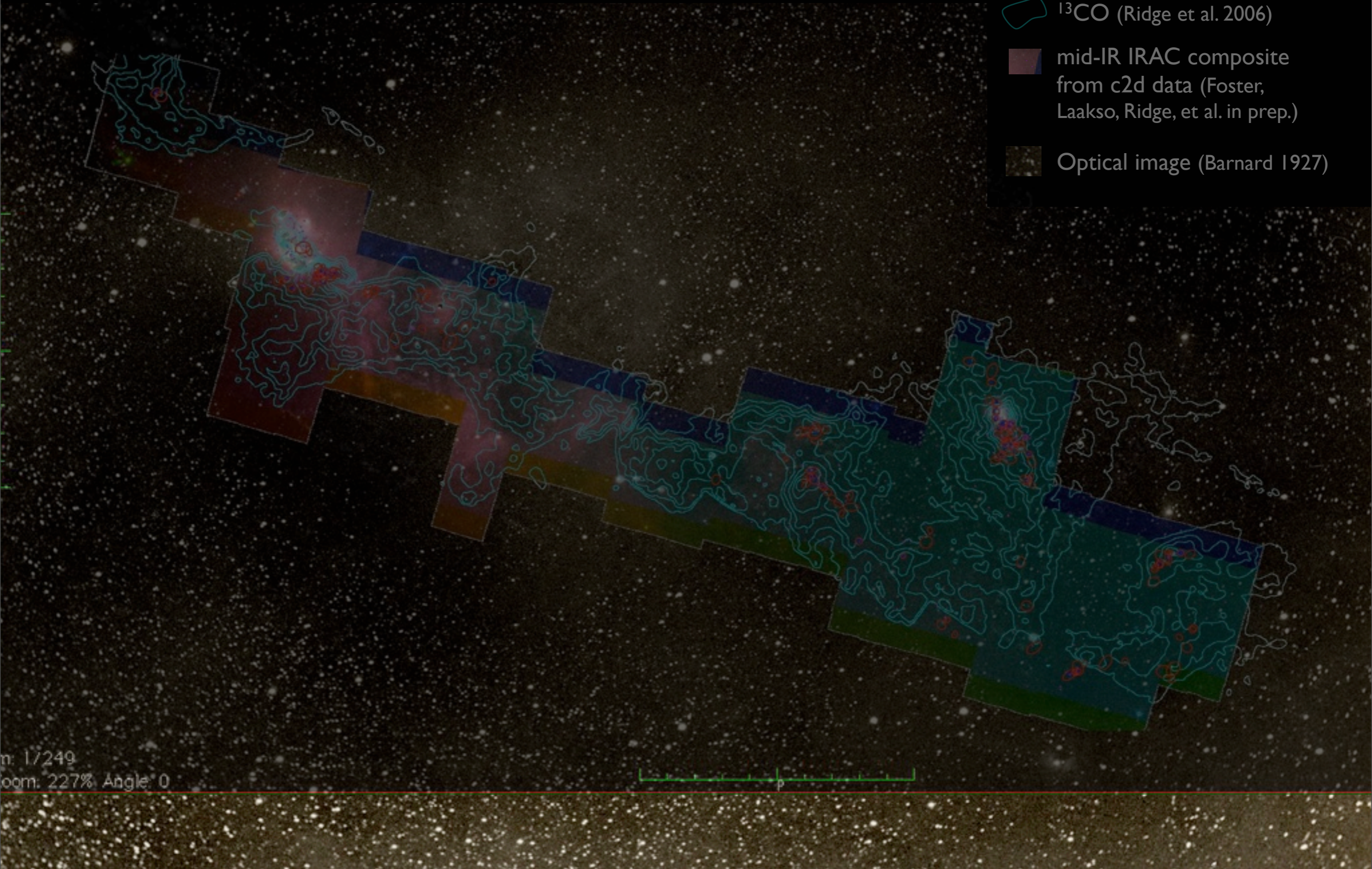
Quiz (and Demo)



COMPLETE Perseus

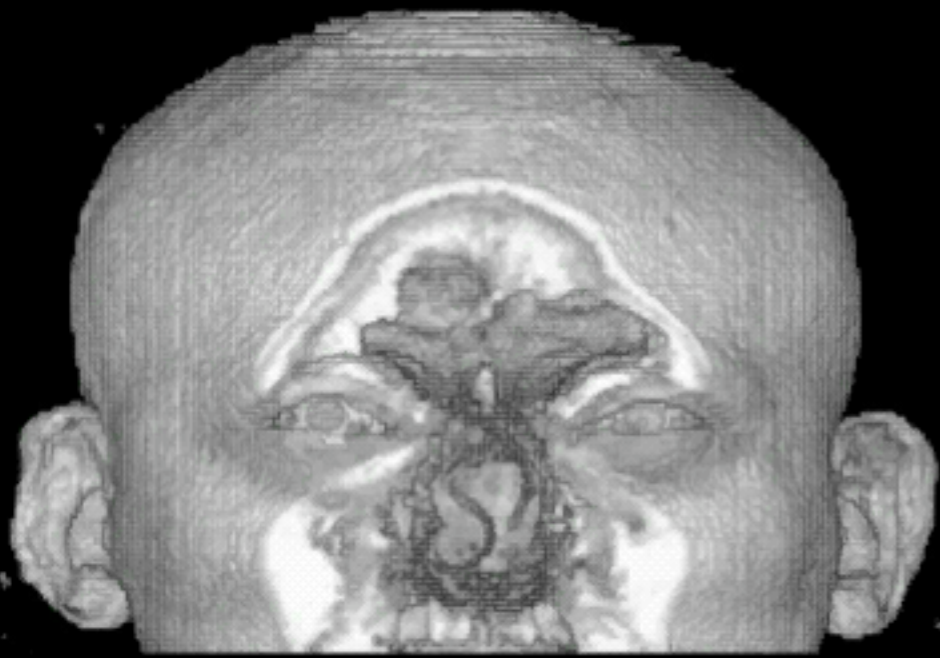
Image size: 1305 x 733
VL: 63 WW: 127

-  mm peak (Enoch et al. 2006)
-  sub-mm peak (Hatchell et al. 2005, Kirk et al. 2006)
-  ^{13}CO (Ridge et al. 2006)
-  mid-IR IRAC composite from c2d data (Foster, Laakso, Ridge, et al. in prep.)
-  Optical image (Barnard 1927)



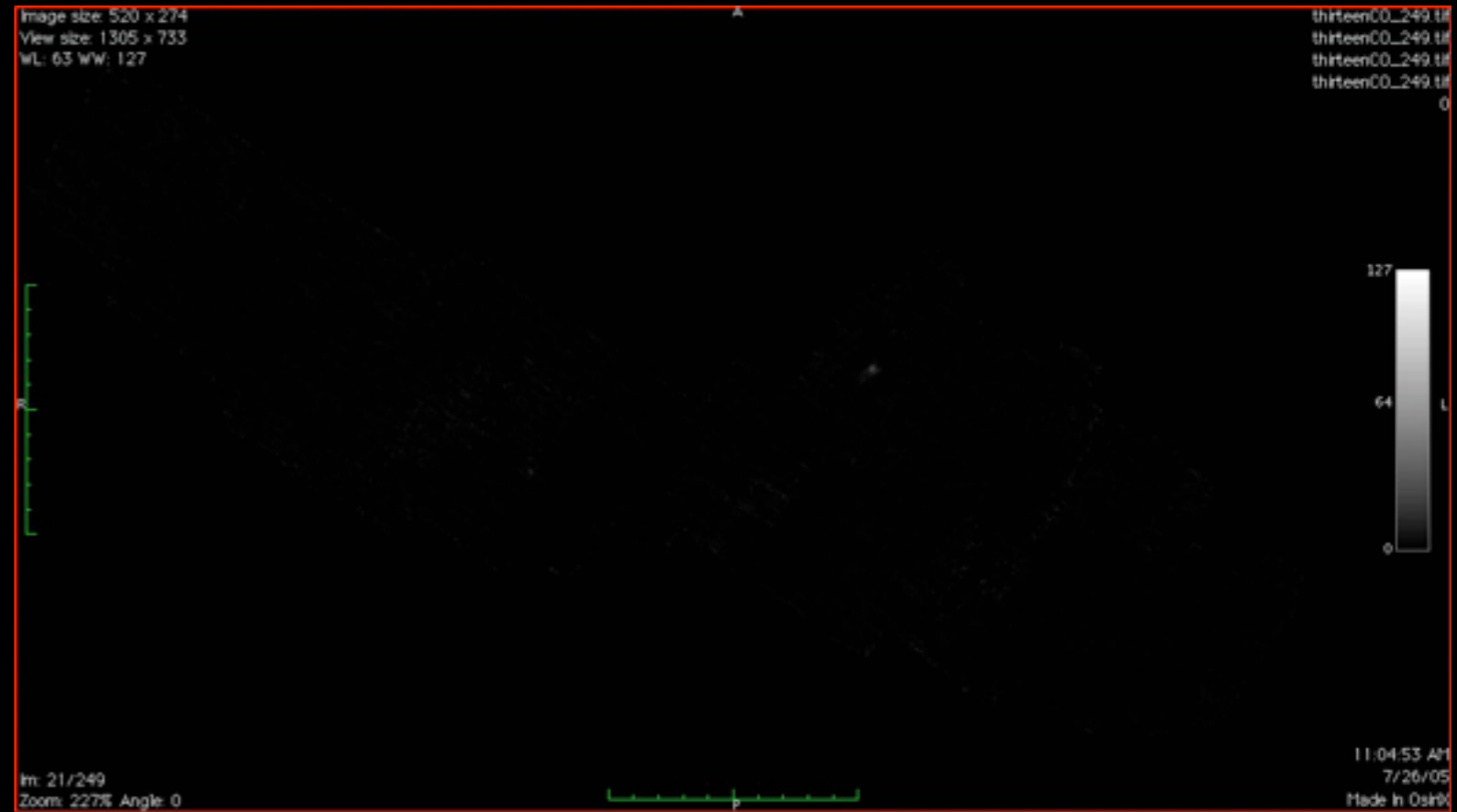
“Astronomical Medicine”

“KEITH”



“z” is depth into head

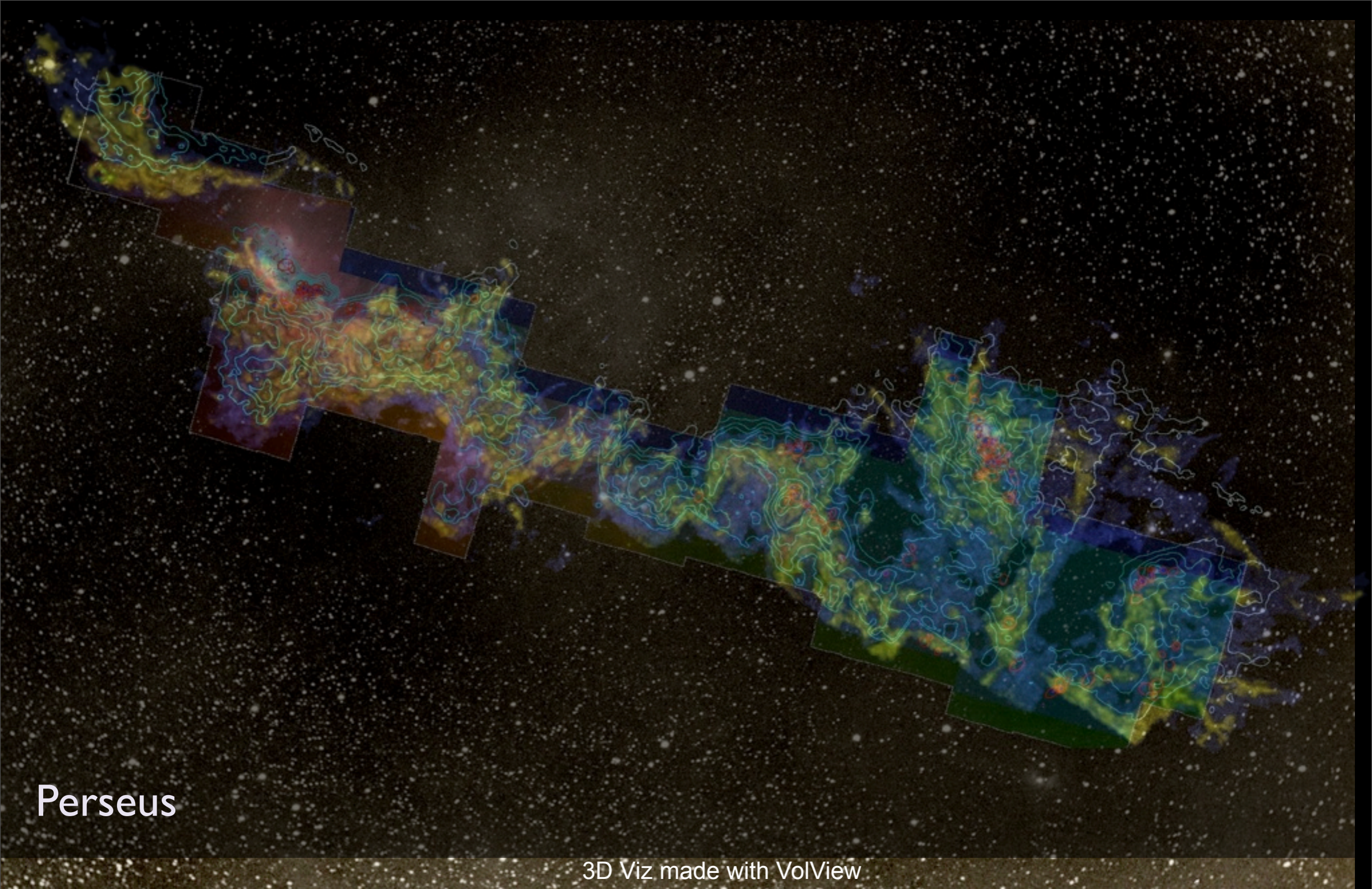
“PERSEUS”



“z” is line-of-sight velocity

(This kind of “series of 2D slices view” is known in the Viz as “the grand tour”)





Perseus

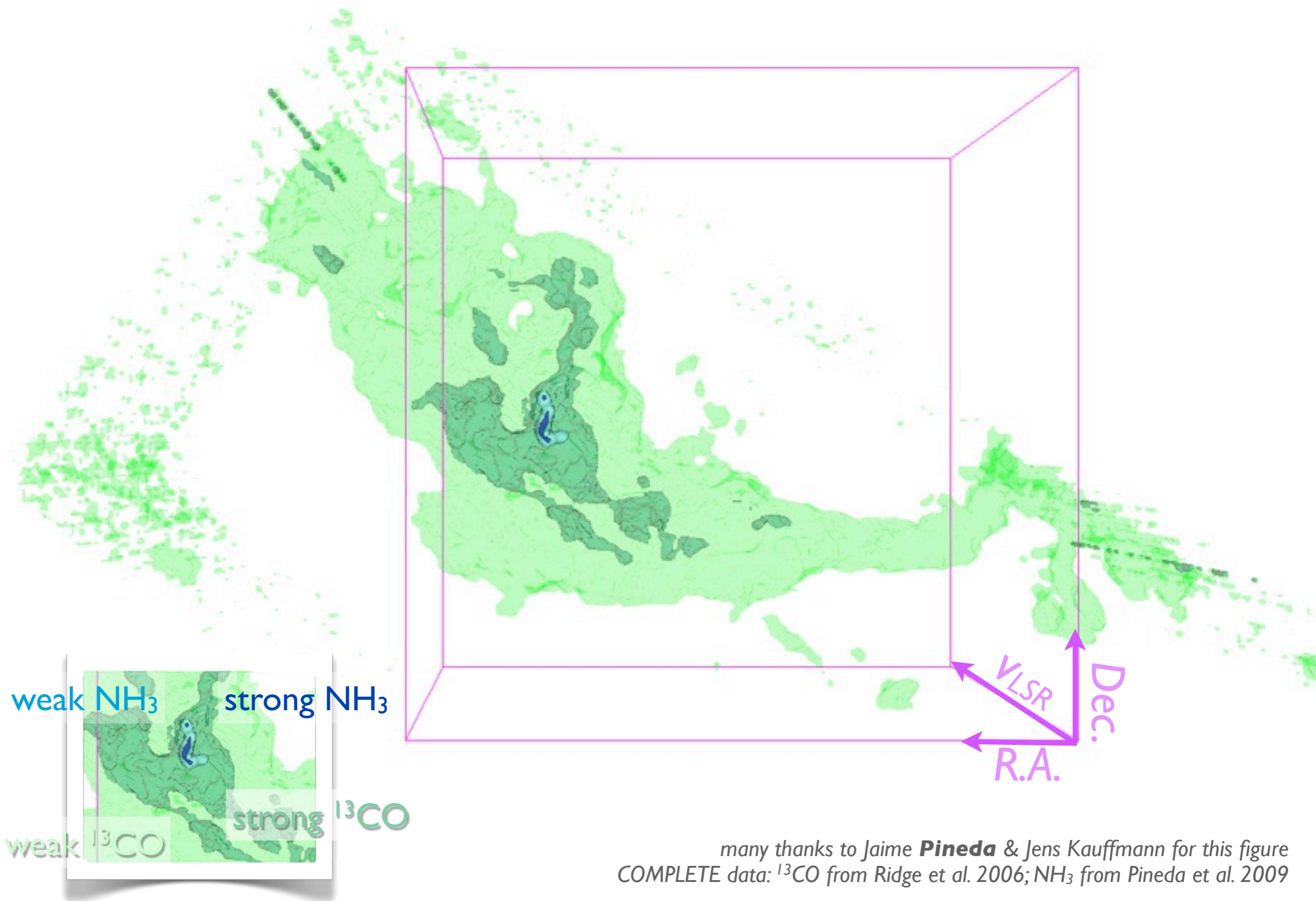
3D Viz made with VolView

AstronomicalMedicine@iig

COMPLETE

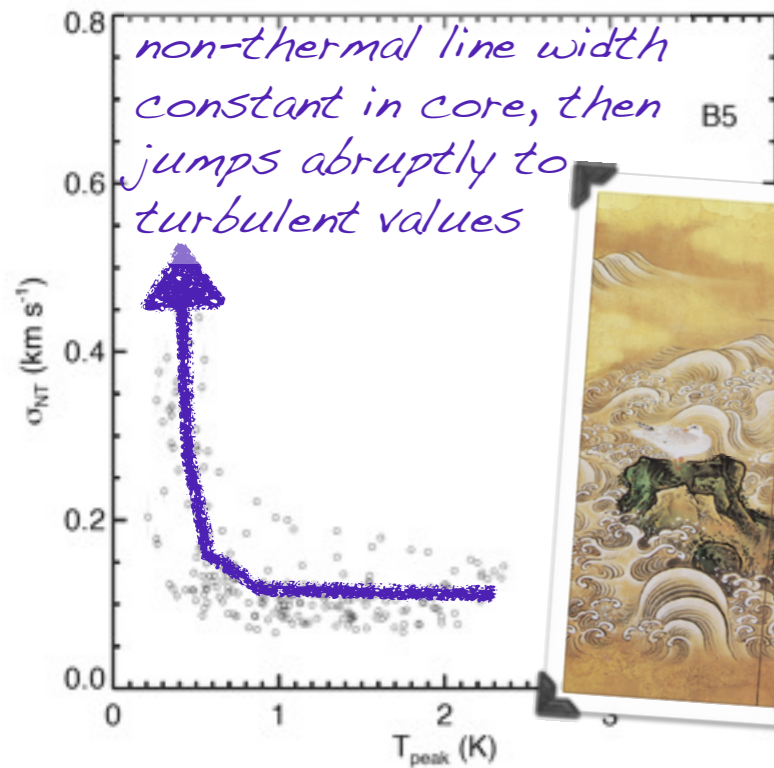
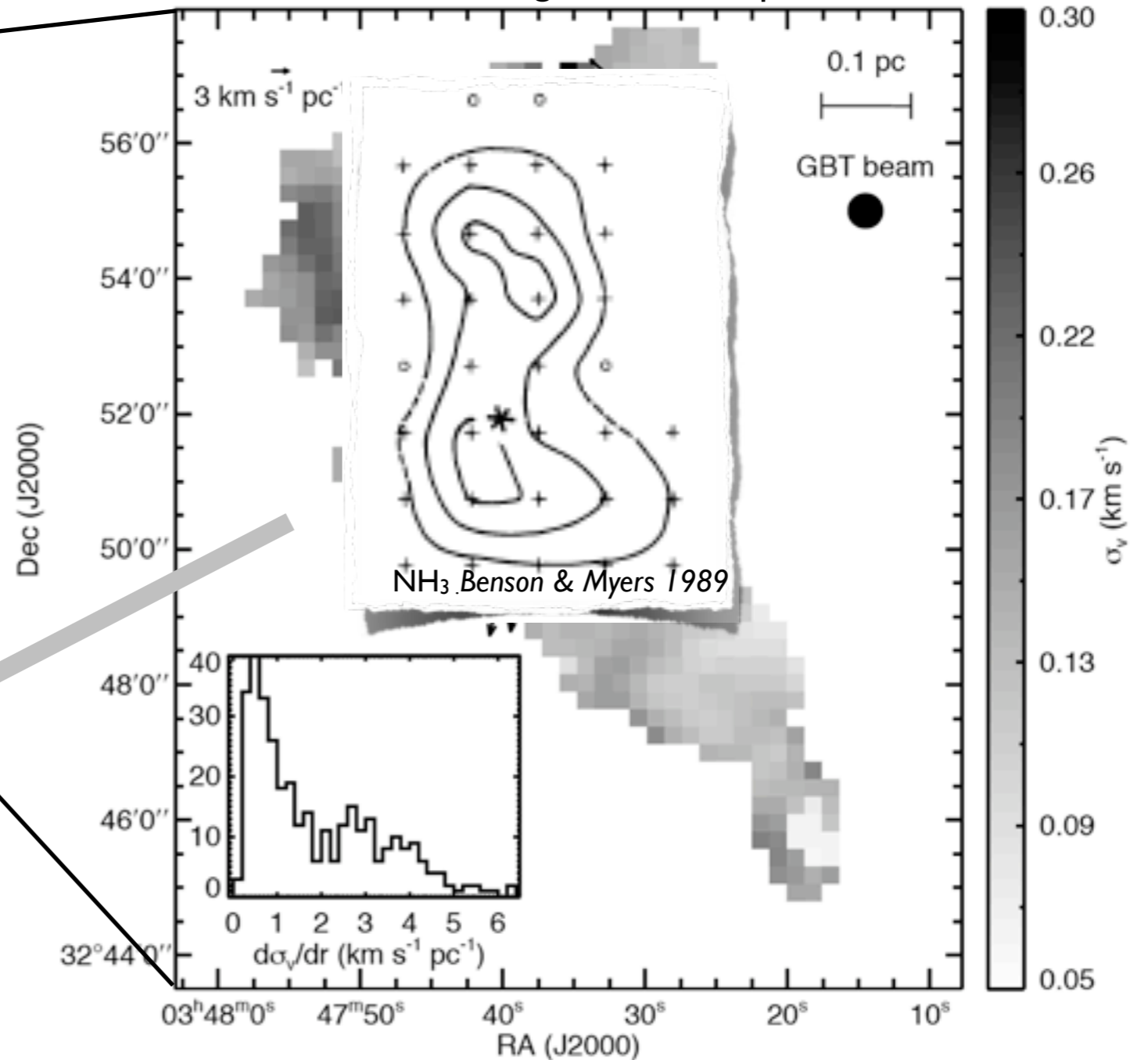
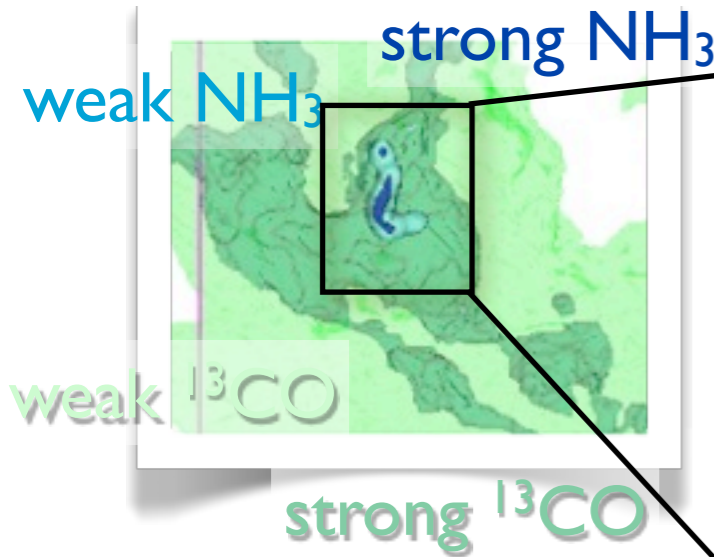
Monday, November 16, 2009

p - p - v structure of the B5 region in Perseus



A Rapid Transition to Coherence in Dense Cores

greyscale shows NH_3 velocity dispersion, arrows show gradient in dispersion



These are the new GBT NH_3 observations of the B5 core, which Jaime Pineda spoke about yesterday

The future is here: 3D PDF

LETTERS

A role for self-gravity at multiple length scales in the process of star formation

Alysa A. Goodman^{1,2}, Dik W. Rieuweveldy^{1,2}, Michelle A. Barkin¹, Jonathan S. Foster¹, Michael Habibi^{1,3}, Jens Kauffmann^{1,2} & James E. Proctor¹

Self-gravity plays a decisive role in the final stages of star formation, where dense cores (size ~ 0.1 parsecs) build molecular clouds collapse to form star-gas disk systems¹. But self-gravity's role at earlier times (and on larger length scales, such as ~ 1 parsec) is unclear: some molecular cloud simulations that do not include self-gravity suggest that turbulent fragmentation alone is sufficient to create a mass distribution of structures that resembles, at least in part, the observed star formation rate². However, other simulations (including those that do include self-gravity) suggest that self-gravity plays a significant role over the full range of possible scales probed by CO observations in the L1448 molecular cloud, but not everywhere in the observed region. In particular, more than 80 per cent of the compact 'pre-main-sequence' cores in the 'dense core' region are predicted to be self-gravitating by the end of the simulation's self-gravitating phase³. As these peaks mark the location of already-forming stars, or of those probably about to form, self-gravitating cores would constitute a critical condition for their existence. Turbulent fragmentation simulations without self-gravity and/or unphysical initial conditions—such as zero initial velocity and zero initial magnetic field—may yield stars and velocity power spectra very similar to what is observed in clouds like L1448. But a development of such a simulation 'shows that nearly all the gas in it clumps more than in the observations' appears to be self-gravitating, a potentially significant role for gravity to 'seed' self-gravitating simulations suggests inconsistency to simulation assumptions and output, and that it is necessary to include self-gravity in any realistic simulation of the star-formation process in self-gravitating clouds.

Spectral-line mapping shows whole molecular clouds (typically tens to hundreds of parsecs across, and surrounded by atomic gas) to be marginally self-gravitating⁴. When attempts are made to further break down clouds into pieces using 'fragmentation' routines, some self-gravitating structures are also found on subcloud scales⁵. But no observational study to date has successfully used any spectral-line data cube to study the role of self-gravity versus a function of scale and conditions, within an individual region. Most past structure identification in molecular clouds has been explicitly non-hierarchical, which makes difficult the quantification of physical conditions on multiple scales using a single data set. Consider, for example, the often-used algorithm CLUMFIND^{6,7}. Its three-dimensional CO spectral-line data cubes, CLUMFIND outputs as a hierarchical segmentation algorithm, identifying local maxima in the position-position-velocity (p-p-v) cube and comparing nearby maxima to each local maximum. Figure 1 shows a two-dimensional CO data cube of L1448, an example star-forming region, and Fig. 2 compares CLUMFIND's segmentation with that of a new algorithm that does not offer hierarchical output as

employing features on an explicit, significant criterion based between processes that typically either depend on the source change or occur over a much smaller 'pathological' feature. Instead, the maximum of the feature is used to identify the feature. This feature is then used to identify the feature.



Figure 1: Near infrared image of the L1448 star-forming region with contours overlaid. The contours show the distribution of the surface indicated by the dendrogram. The image shows a complex, multi-scale structure with various sized clumps and filaments.

Figure 2: Comparison of the 'dendrogram' and 'CLUMFIND' feature-identification algorithms as applied to CO emission from the L1448 region of Perseus. A 3D visualization of the surface indicated by the dendrogram shows a 3D visualization of the surface indicated by the dendrogram. The dendrogram shows a 3D visualization of the surface indicated by the dendrogram. The dendrogram shows a 3D visualization of the surface indicated by the dendrogram.

Figure 3: Schematic illustration of the dendrogram process. The construction of a dendrogram from a hierarchical one-dimensional feature profile (black). The dendrogram (blue) can be constructed by 'merging a set of points (for example the light purple dots) in one dimension, a plane curve in two dimensions, and an isosurface in three dimensions. The dendrogram of 3D data shows in Fig. 3 is the direct analogue of the tree shown here, only constructed from 'isometric' rather than 'point' intersections. It has been carried and returned to the representation as a 2D plot, as fully representing dendrograms for 3D data cubes would require four dimensions.

LETTERS

LETTERS

3D visualization of the surface indicated by the dendrogram shows a 3D visualization of the surface indicated by the dendrogram. The dendrogram shows a 3D visualization of the surface indicated by the dendrogram. The dendrogram shows a 3D visualization of the surface indicated by the dendrogram.

Figure 2: Comparison of the 'dendrogram' and 'CLUMFIND' feature-identification algorithms as applied to CO emission from the L1448 region of Perseus. A 3D visualization of the surface indicated by the dendrogram shows a 3D visualization of the surface indicated by the dendrogram. The dendrogram shows a 3D visualization of the surface indicated by the dendrogram. The dendrogram shows a 3D visualization of the surface indicated by the dendrogram.

Figure 3: Schematic illustration of the dendrogram process. The construction of a dendrogram from a hierarchical one-dimensional feature profile (black). The dendrogram (blue) can be constructed by 'merging a set of points (for example the light purple dots) in one dimension, a plane curve in two dimensions, and an isosurface in three dimensions. The dendrogram of 3D data shows in Fig. 3 is the direct analogue of the tree shown here, only constructed from 'isometric' rather than 'point' intersections. It has been carried and returned to the representation as a 2D plot, as fully representing dendrograms for 3D data cubes would require four dimensions.

LETTERS

LETTERS

3D visualization of the surface indicated by the dendrogram shows a 3D visualization of the surface indicated by the dendrogram. The dendrogram shows a 3D visualization of the surface indicated by the dendrogram. The dendrogram shows a 3D visualization of the surface indicated by the dendrogram.

Figure 4: The fraction of self-gravitating volume as a function of scale in L1448 and a comparison simulation. The fraction of volume in the L1448 region contained within larger-scale self-gravitating structures, but only a few percent of self-gravitating volume, is shown in red. The fraction of self-gravitating volume in the L1448 region is shown in blue. The fraction of self-gravitating volume in the L1448 region is shown in blue. The fraction of self-gravitating volume in the L1448 region is shown in blue.

Figure 5: Schematic illustration of the dendrogram process. The construction of a dendrogram from a hierarchical one-dimensional feature profile (black). The dendrogram (blue) can be constructed by 'merging a set of points (for example the light purple dots) in one dimension, a plane curve in two dimensions, and an isosurface in three dimensions. The dendrogram of 3D data shows in Fig. 3 is the direct analogue of the tree shown here, only constructed from 'isometric' rather than 'point' intersections. It has been carried and returned to the representation as a 2D plot, as fully representing dendrograms for 3D data cubes would require four dimensions.

LETTERS

LETTERS

3D visualization of the surface indicated by the dendrogram shows a 3D visualization of the surface indicated by the dendrogram. The dendrogram shows a 3D visualization of the surface indicated by the dendrogram. The dendrogram shows a 3D visualization of the surface indicated by the dendrogram.

Figure 4: The fraction of self-gravitating volume as a function of scale in L1448 and a comparison simulation. The fraction of volume in the L1448 region contained within larger-scale self-gravitating structures, but only a few percent of self-gravitating volume, is shown in red. The fraction of self-gravitating volume in the L1448 region is shown in blue. The fraction of self-gravitating volume in the L1448 region is shown in blue.

Figure 5: Schematic illustration of the dendrogram process. The construction of a dendrogram from a hierarchical one-dimensional feature profile (black). The dendrogram (blue) can be constructed by 'merging a set of points (for example the light purple dots) in one dimension, a plane curve in two dimensions, and an isosurface in three dimensions. The dendrogram of 3D data shows in Fig. 3 is the direct analogue of the tree shown here, only constructed from 'isometric' rather than 'point' intersections. It has been carried and returned to the representation as a 2D plot, as fully representing dendrograms for 3D data cubes would require four dimensions.

COMPLETE Data Coverage Tool

http://www.worldwidetelescope.org/COMPLETE/WWTCoverageTool.htm#

COMPLETE

COMPLETE Data Available

Center on Perseus Center on Ophiuchus Center on Serpens

Full-Cloud Data (Phase I, All Data Available)

Dataset	Show	Perseus	Ophiuchus	Serpens	Link
GBT: HI Data Cube	<input checked="" type="checkbox"/>	✓	✓	∅	Data
IRAS: Av/Temp Maps	<input checked="" type="checkbox"/>	✓	✓	✓	Data
FCRAO: 12CO	<input checked="" type="checkbox"/>	✓	✓	✓	Data
FCRAO: 13CO	<input checked="" type="checkbox"/>	✓	✓	✓	Data
JCMT: 850 microns	<input checked="" type="checkbox"/>	✓	✓	∅	Data
Spitzer c2d: IRAC 1,3 (3.6,5.8 μm)	<input checked="" type="checkbox"/>	✓	✓	✓	Data
Spitzer c2d: IRAC 2,4 (4.5,8 μm)	<input checked="" type="checkbox"/>	✓	✓	✓	Data
CSO/Bolocam: 1.2-mm	<input checked="" type="checkbox"/>	✓	∅	∅	Data
Spitzer MIPS: Derived Dust Map	<input checked="" type="checkbox"/>	✓	∅	∅	Data

Targeted Regions (Phase II, Some Data Not Yet Available)


CTIO/Calar Alto: NIR (J,H,Ks)	<input checked="" type="checkbox"/>	✓	✓	∅	Data
IRAM 30-m: N2H+ and C18O	<input checked="" type="checkbox"/>	✓	∅	∅	Data
IRAM 30-m: 1.1-mm continuum	<input checked="" type="checkbox"/>	✓	∅	∅	Data
Megacam/MMT: r,i,z images	<input checked="" type="checkbox"/>	✓	∅	∅	Data

Catalogs & Pointed Surveys

NH3 Pointed Survey	<input type="checkbox"/>	✓	∅	∅	Data
YSO Candidate list (c2d)	<input type="checkbox"/>	✓	✓	✓	Data

Microsoft Research
WorldWide Telescope

Done

To explore on your own, go to <http://www.cfa.harvard.edu/COMPLETE/>, then click on  and choose to see the Interactive Coverage Tool in either Google Sky or WorldWide Telescope.

Many thanks to Jonathan Foster, Gus Muench & Jonathan Fay (MSR/WWT team) for these tools!